State Key Laboratory of Space Weather
Chinese Academy of Sciences
SIGMA
WEATHER GROUP

Modeling the solar energetic particle transport in the 3D background solar wind

Presenter: Fang Shen[1,2]

Collaborators: Wenwen Wei[1], Zicai Yang[1], Lulu Zhao[3], Yang Wang[2], Pingbing Zuo[2] and Xueshang Feng[1,2]

[1]SIGMA Weather Group, State Key Laboratory of Space Weather, NSSC, CAS, Beijing, China

[2]HIT Institute of Space Science and Applied Technology, Shenzhen, China

[3]Department of Physics and Space Sciences, Florida Institute of Technology, Melbourne, FL , USA

2017-09-21, WG6, ISEST 2017,
Jeju, Republic of Korea

Outline:

- Introduction
- MHD-SEP model
  - MHD Model
  - Particle Transport Model
- Simulation Results and Discussion
  - Uncompressed Solar Wind Conditions
  - Compression Region Conditions
- Summary

Solar Energetic Particle (SEP) events

The Space Environment Center of the National Oceanic and Atmospheric Administration defines a SEP event as the flux of interplanetary particles that exceeds the threshold of 10 pfu during 15 minutes for E >10 MeV.

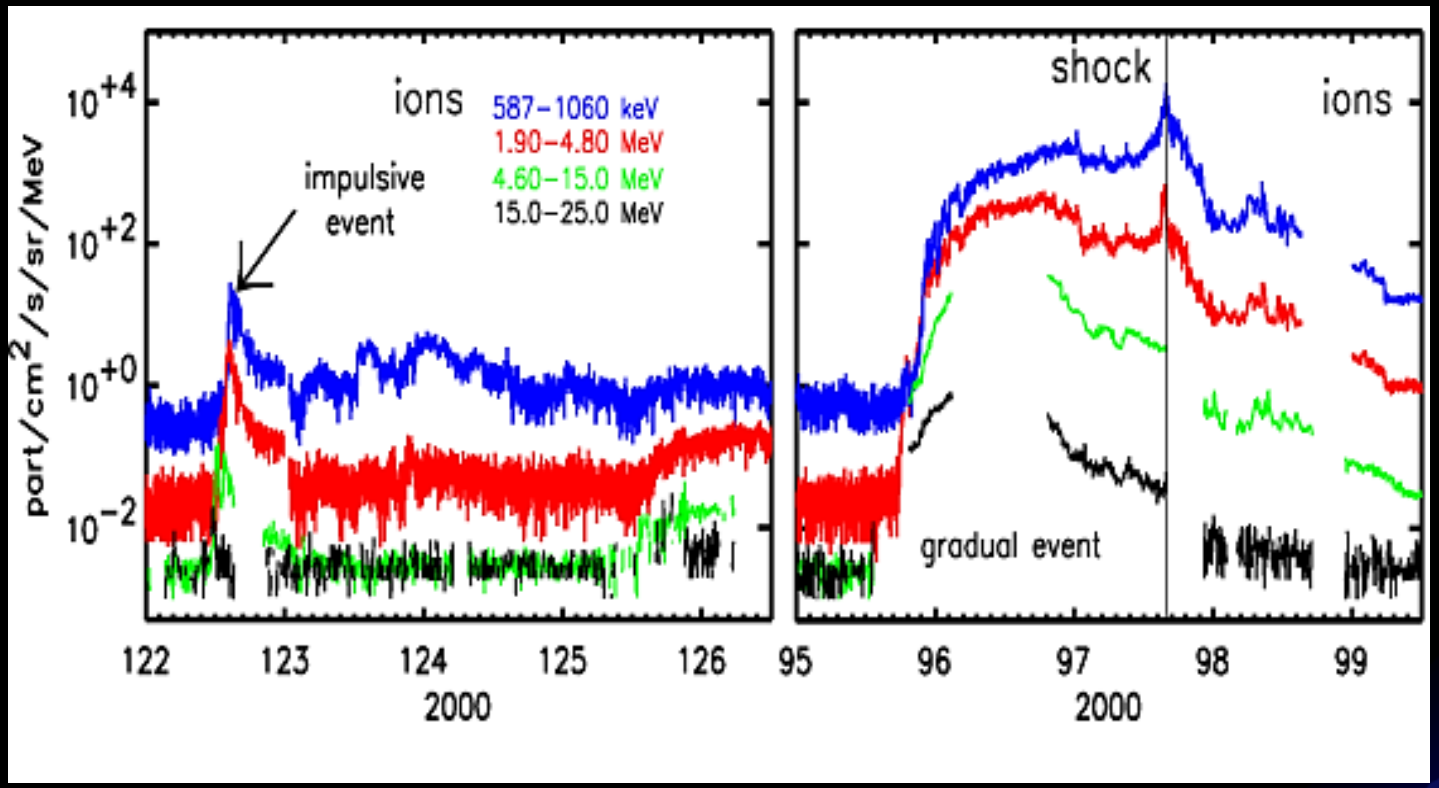

Figure1 Intensity-time profiles of ions for an impulsive (left) and a gradual (right)SEP event of the year 2000 as measured by ACE/EPAM (Gold et al. 1998; hereafter Gol98). The two lower traces (high energy channels) are proton observations from IMP-8/CPME (Sarris et al. 1976; hereafter Sar76).

Modeling SEP Events

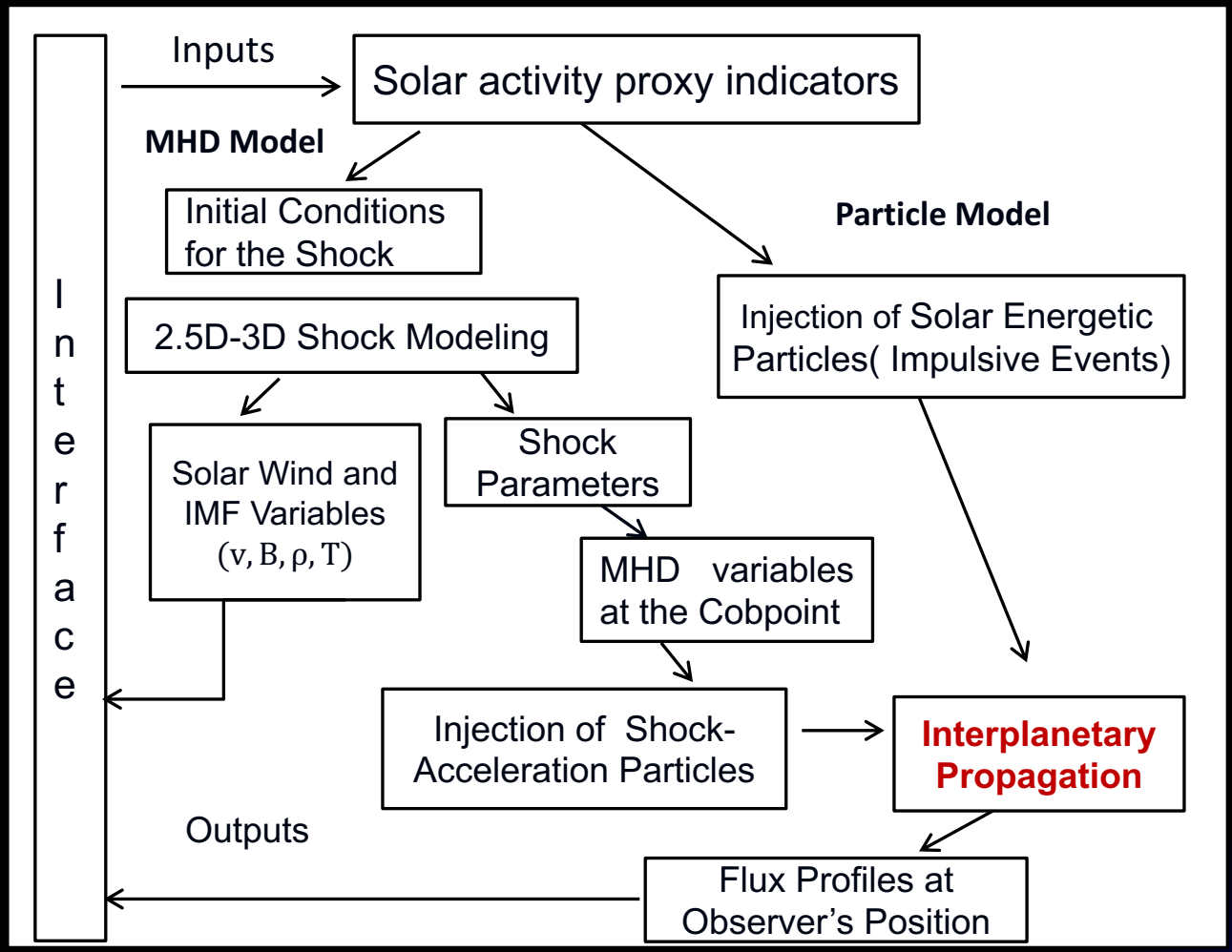

Figure 2 Basic blocks and interfaces of the shock-and-particle model.
(A. Aran, PhD. thesis,2007)

Our purpose:

- Our purpose is to employ the MHD-SEP model to study the transport of SEPs in both the uncompressed solar wind and the compression region;
- For the sake of simplicity, we concentrate on the propagation of high-energy ($E \geq 30$ MeV) SEPs in the 3D background solar wind with no disturbances from shocks or ICMEs.

MHD Model

The ideal MHD equations in a solar corotating frame:

$$\frac{\partial \rho}{\partial t} + \nabla \cdot (\rho \boldsymbol{V}) = 0$$

$$\frac{\partial \rho \boldsymbol{V}}{\partial t} + \nabla \cdot \left[\left(P + \frac{B^2}{2\mu_0} \right) \boldsymbol{I} + \rho \boldsymbol{V}\boldsymbol{V} - \frac{\boldsymbol{B}\boldsymbol{B}}{\mu_0} \right] = -\frac{\rho G M_s}{r^2} \frac{\boldsymbol{r}}{r} + \boldsymbol{f}$$

$$\frac{\partial \boldsymbol{B}}{\partial t} + \nabla \cdot (\boldsymbol{V}\boldsymbol{B} - \boldsymbol{B}\boldsymbol{V}) = 0$$

$$\frac{\partial P}{\partial t} + \nabla \cdot (\rho \boldsymbol{V}) + (\gamma - 1) P \nabla \cdot \boldsymbol{V} = 0$$

The steady state 3D background solar wind is constructed by solving the ideal MHD equations with high resolution TVDLF scheme (Shen et al., JGR, 2011, 2012, 2013, 2014).

MHD Model

- Six-component composite mesh was used to avoid the coordinate singularity near the poles, in order to reduce high numerical dissipation;
- The computational domain of the mesh grid system is:

0.1 AU ≤ r ≤ 8 AU, 0 ≤ ϑ ≤ π,

and 0 ≤ φ ≤ 2π

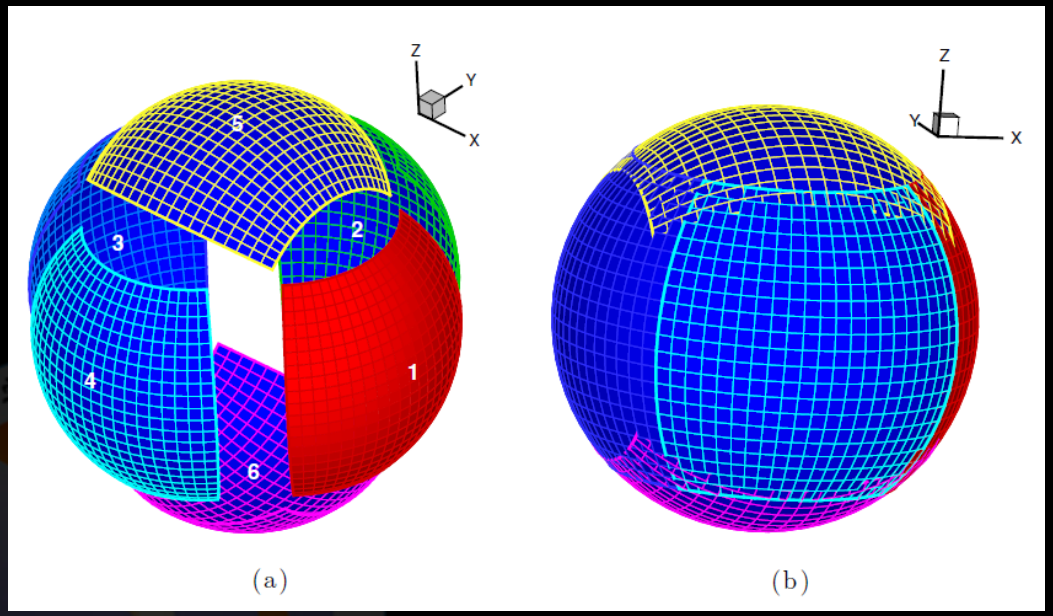

Figure 1. Basic six-component grid: (a) a spherical overset grid and (b) a partition of a sphere into six identical components with partial overlaps. Each component grid is a rectangle in the (ϑ, φ) space (from Feng et al., *APJ*, 2010).

- The artificial diffusive approach is used to reduce the numerical error of $\nabla \cdot \boldsymbol{B}$;
- Inner boundary: 21.5 R_s (~0.1 AU):

  The radial magnetic field (B_r) is provided with the PFSS model;

  The radial flow velocity, V_r (km s^{-1}), is obtained from the WSA model.

Particle Transport Model—Equations

Focused Transport Equation (Fokker-Planck Equation):

$$\frac{\partial f}{\partial t}+(v\mu\boldsymbol{b}+\boldsymbol{V}_{\mathrm{sw}})\cdot\nabla f-\frac{\partial}{\partial\mu}D_{\mu\mu}\frac{\partial f}{\partial\mu}$$
$$+\left[\frac{(1-\mu^2)v}{2L_{\mathrm{B}}}+\frac{\mu(1-\mu^2)}{2}(\nabla\cdot\boldsymbol{V}_{\mathrm{sw}}-3\boldsymbol{bb}:\nabla\boldsymbol{V}_{\mathrm{sw}})\right]\frac{\partial f}{\partial\mu}$$
$$-\left[\frac{1-\mu^2}{2}(\nabla\cdot\boldsymbol{V}_{\mathrm{sw}}-\boldsymbol{bb}:\nabla\boldsymbol{V}_{\mathrm{sw}})+\mu^2\boldsymbol{bb}:\nabla\boldsymbol{V}_{\mathrm{sw}}\right]p\frac{\partial f}{\partial p}=0$$

Where $f(\mathbf{x}, \mu, p, t)$ is the gyro phase-averaged distribution function of SEPs as a function of spatial location $\boldsymbol{x}$, particle momentum p, pitch-angle cosine μ, and time t. v is the particle speed, $\boldsymbol{b}$ is the magnetic field unit vector, $\boldsymbol{V}_{\mathrm{sw}}$ is the solar wind velocity, $D_{\mu\mu}$ is the pitch-angle diffusion coefficient, and $L_B = -(\boldsymbol{b}\cdot\nabla \ln B)^{-1}$ is the magnetic focusing length

Particle Transport Model—Equations

The adiabatic cooling effect is described by:

$$\frac{dp}{dt} = -p\left[\frac{\mu}{v}\boldsymbol{b}\cdot\left(\frac{\partial \boldsymbol{V}_{SW}}{\partial t} + \boldsymbol{V}_{SW}\cdot\nabla\boldsymbol{V}_{SW}\right) + \frac{1-\mu^2}{2}\left(\nabla\cdot\boldsymbol{V}_{SW} - \boldsymbol{bb}:\nabla\boldsymbol{V}_{SW}\right) + \mu^2\boldsymbol{bb}:\nabla\boldsymbol{V}_{SW}\right]$$

and the time evolution of μ is written as

$$\frac{d\mu}{dt} = \mu\boldsymbol{b}\cdot\left(\frac{\partial \boldsymbol{b}}{\partial t} + \mathbf{V}_{SW}\cdot\nabla\boldsymbol{b}\right) - \frac{1-\mu^2}{v}\boldsymbol{b}\cdot\left(\frac{\partial \boldsymbol{V}_{SW}}{\partial t} + \boldsymbol{V}_{SW}\cdot\nabla\boldsymbol{V}_{SW}\right) + \frac{\left(1-\mu^2\right)v}{2L_B}$$
$$+ \frac{\mu\left(1-\mu^2\right)}{2}\left(\nabla\cdot\mathbf{V}_{SW} - 3\boldsymbol{bb}:\nabla\boldsymbol{V}_{SW}\right)$$

Particle Transport Model—Equations

Time-backward stochastic differential equations:

(M. Zhang et al., *APJ*, 2009)

$$d\boldsymbol{x}(s) = -(v\mu(s)\boldsymbol{b} + \boldsymbol{V}_{\mathrm{sw}})ds$$

$$d\mu(s) = \sqrt{2\max(D_{\mu\mu},0)}dw(s) + \left[\frac{\partial D_{\mu\mu}}{\partial\mu} - \frac{\left(1-\mu^2(s)\right)v}{2L_{\mathrm{B}}} - \frac{\mu(s)\left(1-\mu^2(s)\right)}{2}\left(\nabla\cdot\boldsymbol{V}_{\mathrm{sw}} - 3\boldsymbol{bb}:\nabla\boldsymbol{V}_{\mathrm{sw}}\right)\right]ds$$

$$dp(s) = \left[\frac{1-\mu^2(s)}{2}\left(\nabla\cdot\boldsymbol{V}_{\mathrm{sw}} - \boldsymbol{bb}:\nabla\boldsymbol{V}_{\mathrm{sw}}\right) + \mu^2\boldsymbol{bb}:\nabla\boldsymbol{V}_{\mathrm{sw}}\right]p(s)ds$$

where $dw(s)$ is a Wiener process as a function of s which is the time running backward. $dw(s)$ can be generated by random numbers with a Gaussian distribution with a standard deviation.

- The simulation of stochastic processes starts at: **x(0) = x,** ***μ(0) = μ,*** and ***p(0) = p*** at initial backward time *s = 0* at time *t*.
- The equations are solved with an Euler scheme as the time running backward.

Particle Transport Model—Boundary Conditions

The boundary value is a function of time t, particle momentum p, as well as solar longitude φ and colatitude θ if an event has a limited coverage on the Sun.

$$f_{\mathrm{b}}(\boldsymbol{x},\mu,p,t)\big|_{r=R_s} = \frac{p^{-\gamma}}{t} e^{-\left(\frac{T_c}{t}+\frac{t}{T_l}\right)} a(\varphi,\theta)$$

1. Rs is the radial distance at which SEPs are released into the system,
2. γ is the spectral index of source particles,
3. T_c and T_l are the time constants controlling the time profile of particle release from the solar corona,
4. $a(\varphi, \theta)$ is a function specifying the longitudinal and latitudinal dependence of SEP source strength.

The solution is an average of its values at the exit point of simulated process:

$$f(\boldsymbol{x},\mu,p,t) = \frac{\sum_{i=1}^{N} f_{\mathrm{b}}(\boldsymbol{x}_e,\mu_e,p_e,t_e)}{N}$$

Model Parameters Used in the Parker magnetic field & MHD background simulations

Parameters	Formula	Initial Values
Inner Boundary	$\mathrm{r} = R_s$	$R_s = 0.12\mathrm{AU}$
Outer Boundary	$\mathrm{r} = R_0$	$R_0 = 8\mathrm{AU}$
Solar Rotation	$\Omega = 2\pi/\mathrm{T}$	$\mathrm{T} = 27.27\ \mathrm{day}$
Solar Wind	$\boldsymbol{V_{sw}} = V_{\mathrm{sw}}\boldsymbol{e}_r$	$V_{\mathrm{sw}} = 400\mathrm{km}\cdot\mathrm{s}^{-1}$
Parker Magnetic Field	$\boldsymbol{B} = \frac{B_0}{r^2}\boldsymbol{e}_r - \frac{B_0\Omega\sin\theta}{rV_{sw}}\boldsymbol{e}_\varphi$	$B_0 = 3.54\mathrm{nT\ AU}^2$
Pitch Angle Diffusion	$D_{\mu\mu} = D_0(1-\mu^2)\mathrm{v}p^{-b_1}(h+\lvert\mu\rvert^{q-1})\kappa(\mathrm{x})$	D_0 is constant $b_1 = \frac{2}{3}, \mathrm{h} = 0.2, \mathrm{q} = 5/3$ $\kappa(\mathrm{x}) = \cos^2\psi = (B_r/B)^2$

MHD-SEP model

➢ The combination---Grid of Background Field:

Grid Number: 501(r) × 181(θ) × 361 (φ)

Radial grid with equal ratio: $r_i = r_{i-1}+qr_{i-1}(i=1,2,...,N_r)$

Latitudinal grid with same size: $\theta_j =(j-1)\cdot\pi/(N_\theta-1)(j=1,2,...,N_\theta)$

Longitudinal grid with same size: $\varphi_k =(k-1)\cdot2\pi/(N_\varphi-1)(k=1,2,...,N_\varphi)$

where q is equal-ratio coefficient, N_r , N_θ and N_φ represent the mesh numbers in the radial, meridional and azimuthal direction, respectively.
Here N_r=501, N_θ =181 and N_φ=361.

MHD-SEP model

➢ The combination---the reference frames:

- ✓ The momentum, pitch angle and particle speed in the transport equation are defined in the solar wind frame, while the spatial coordinates and solar wind speed are defined in the fixed reference frame.
- ✓ The background solar wind obtained in the solar corotating frame is still time-dependent in the fixed frame. Although time-dependent terms exist in dp/dt and $d\mu/dt$, they can be excluded due to they are minor terms in comparison with other terms.
- ✓ For a fixed point, φ_c is assumed to equal to φ_f at the initial time in both frames, then $\varphi_c = \varphi_f - \Omega \Delta t$ after time Δt.
- ✓ Assuming X-axis in solar corotating frame is coincided with that in the fixed frame, and the background at the time (t-s) is needed when particles run backward. A rotation in longitudinal direction is needed to get the distribution at time (t-s), then we can get the transformed results.
- ✓ The solar wind speed and magnetic field can be derived from the Lorentz transformation.

MHD-SEP model

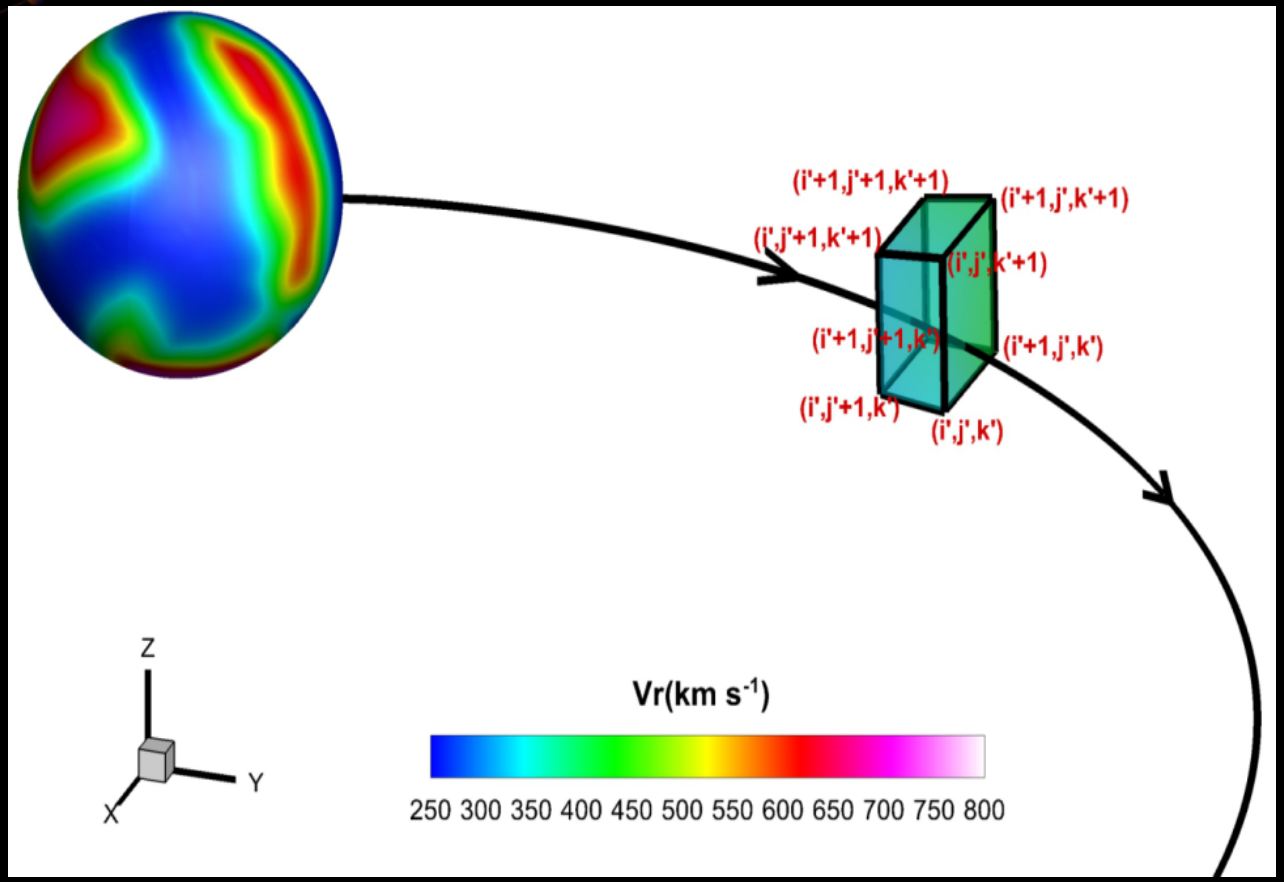

- **Position of particles:** $(r_{i'}, \vartheta_{j'}, \varphi_{k'})$

The subscripts :

$i'=\mathrm{int}(\log(r_{i'}/r_1)/\log(q))+1$

$j'=\mathrm{int}(\theta_{j'}(N_\theta-1)/\pi)+1$

$k'=\mathrm{int}(\varphi_{k'}(N_\varphi-1)/2\pi)+1$

- **The data on the eight adjacent grid points, as marked by *i*', *j*' and *k*', are used to calculate the background parameters.**

Figure4 Illustration of the grid points used in the model. The spherical shell represents the inner boundary of the model, with the color denotes the solar wind speed that is derived from the WSA model. The black solid line with arrow infers the magnetic field line.

The trajectory of a sample stochastic process

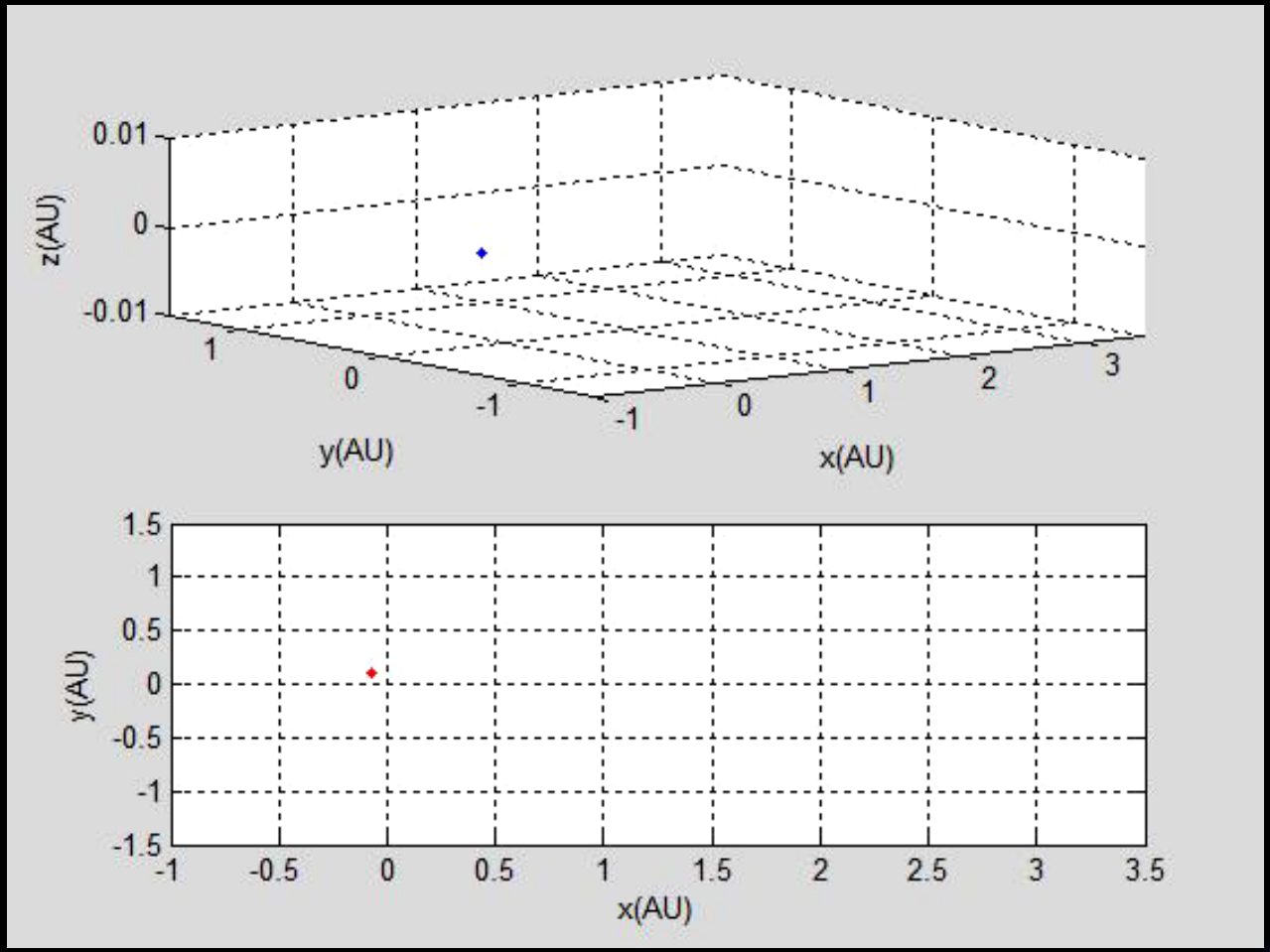

Figure 5 3D and 2D views of how the particle move in the MHD background.

Uncompressed Solar Wind Conditions

The observer： $(r, \theta, \varphi) = (1, 90^o, 0^o)$

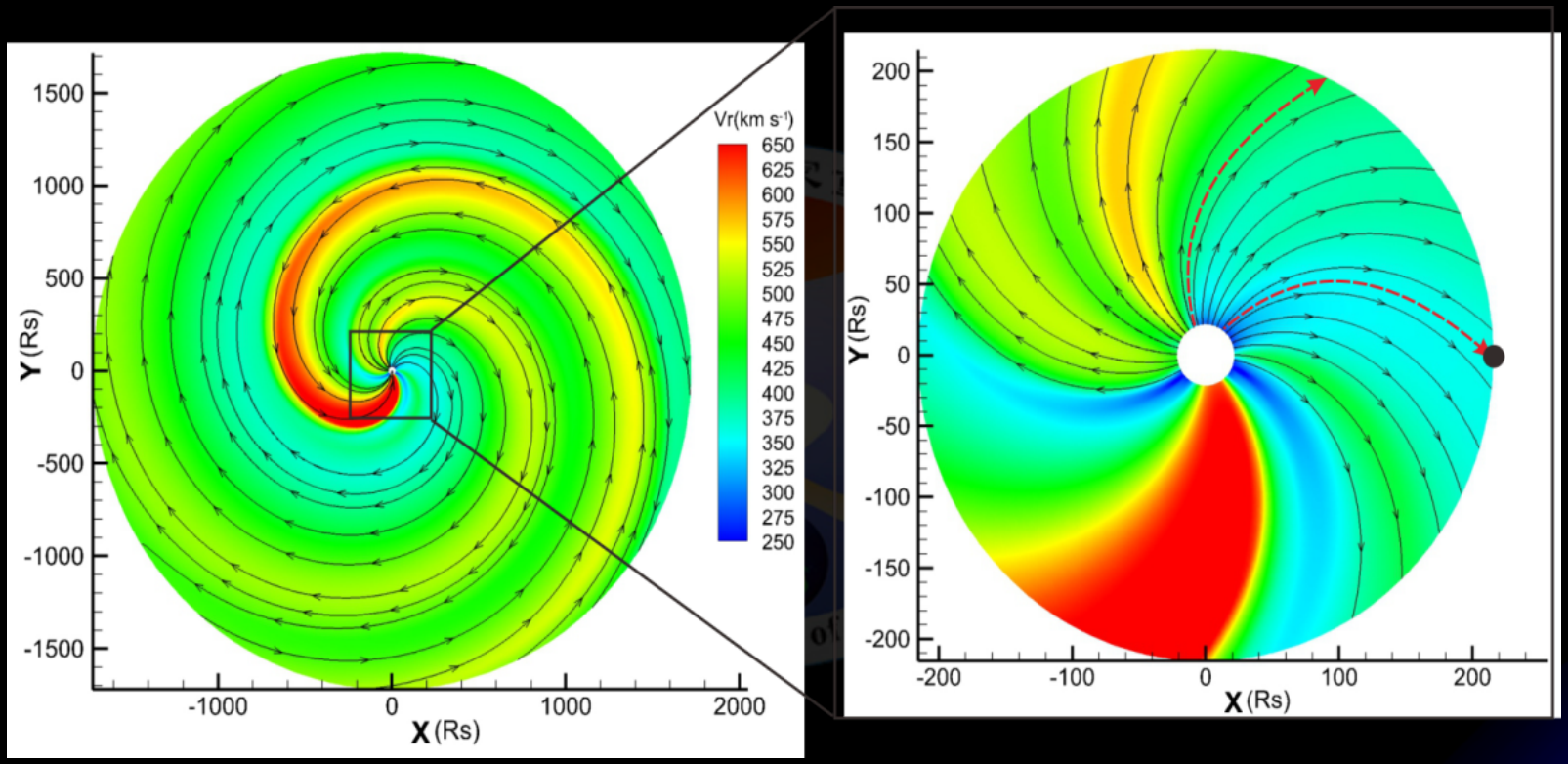

Figure 6 The distribution of the calculated MHD steady radial speed Vr (km s^{-1}) for CR2066 within 8 AU (left panel) and 1 AU (right panel) in the ecliptic plane. The color contours in the left panel represent the radial solar wind speed. Streamlines and the black solid circle in the right panel denote the magnetic field lines and the observation point, respectively. The region that is between the two red dashed lines in right panel is the uncompressed solar wind region.

Uncompressed Solar Wind Conditions

The observer： $(r, \theta, \varphi) = (1, 90^o, 0^o)$

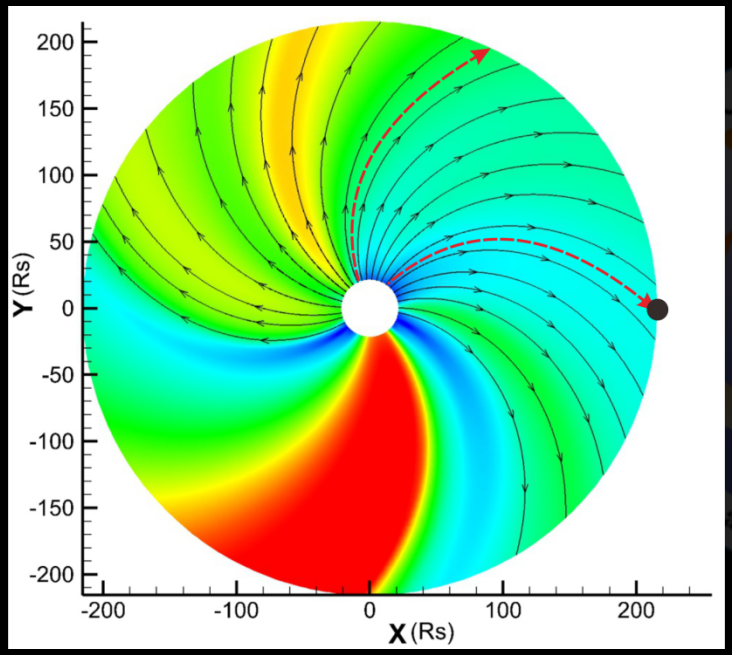

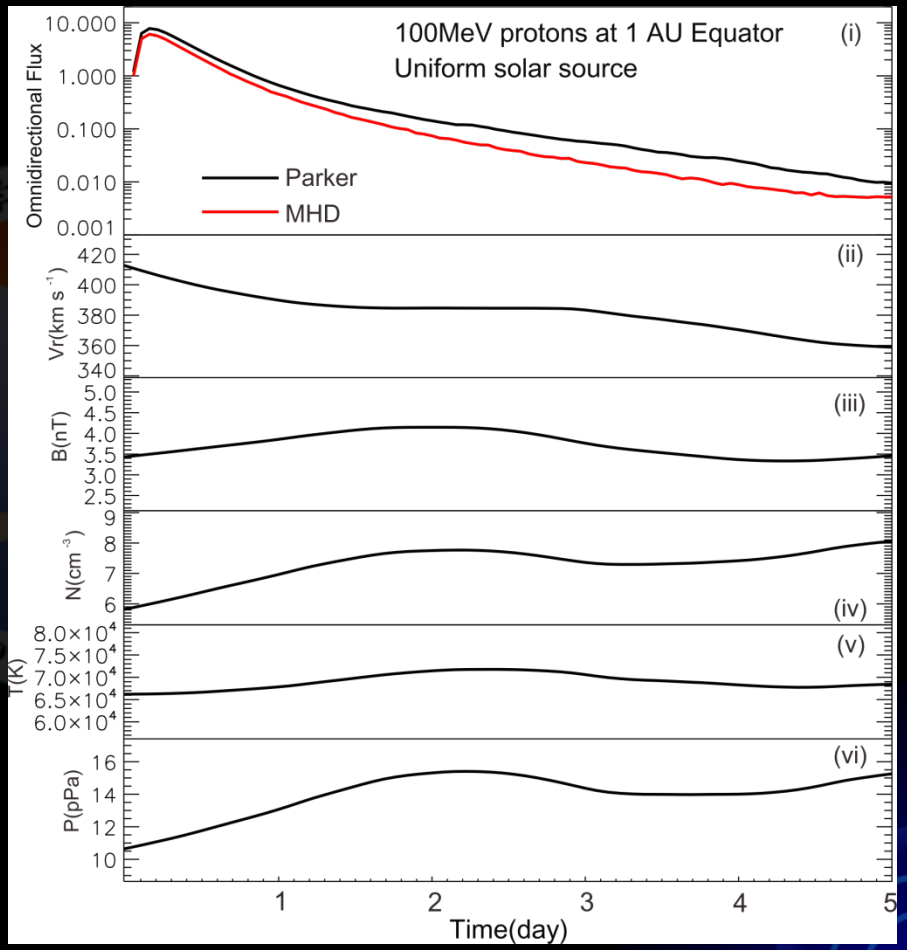

Figure 7. Illustration of omnidirectional flux with different background field and solar wind parameters under uncompressed solar wind conditions.

Compression Region Conditions

The observer： $(r, \theta, \varphi) = (1, 90^o, 90^o)$

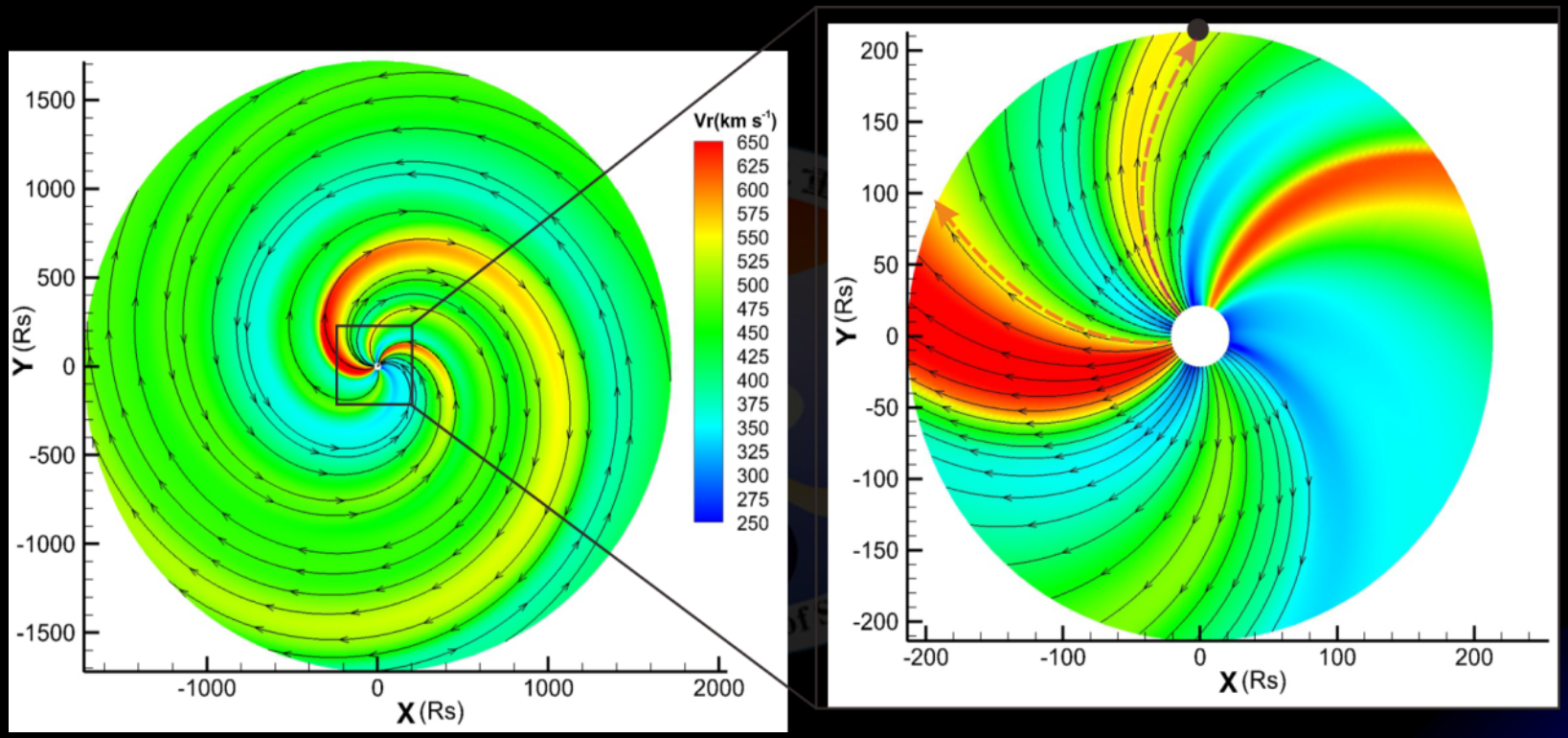

Figure 8 The distribution of the calculated MHD steady radial speed Vr (km s^{-1}) for CR2145 within 8 AU (left panel) and 1 AU (right panel) in the ecliptic plane. The color contours in the left panel represent the radial solar wind speed. Streamlines and the black solid circle in the right panel denote the magnetic field lines and the observation point, respectively. The region that is between the two red dashed lines in right panel is the compression region.

Compression Region Conditions

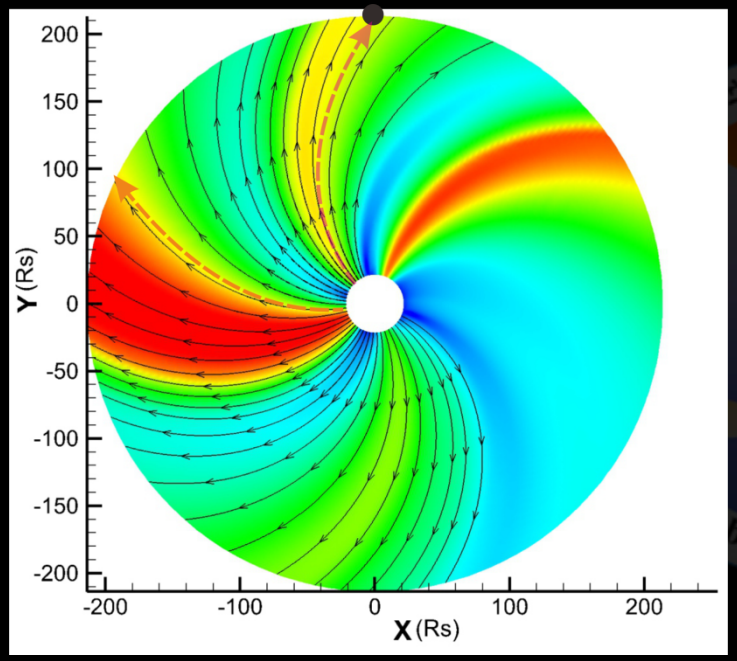

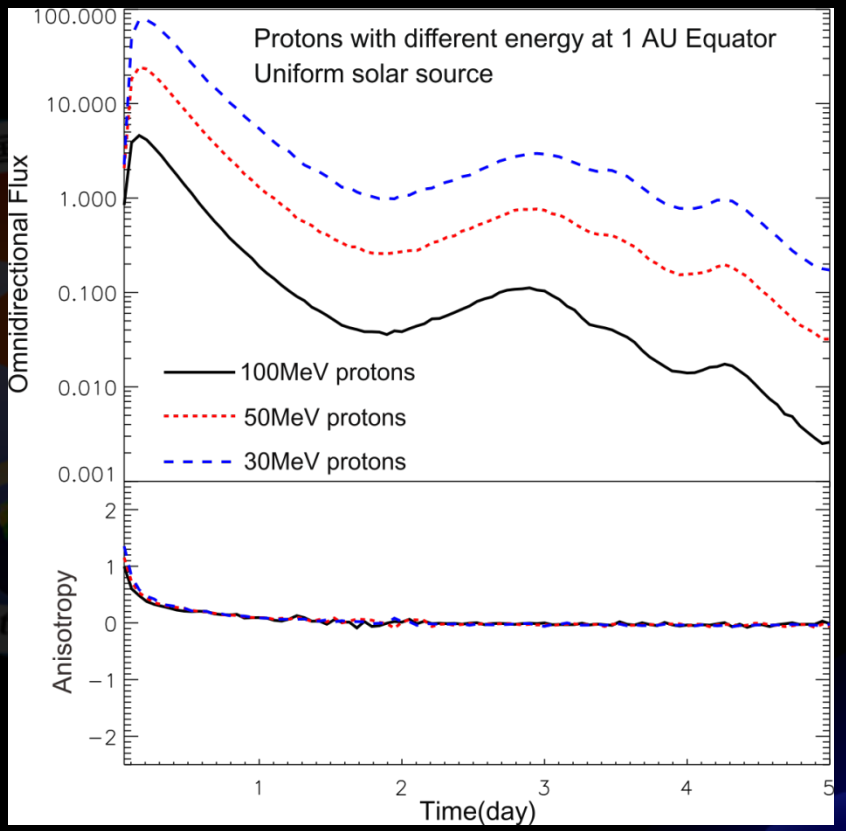

Figure 9 The comparison of omnidirectional flux and anisotropy at three different energies with the same simulated background field.

Discussion—Adiabatic cooling effect

$$dp(s) = \left[\frac{1-\mu^2(s)}{2} \left(\nabla \cdot \boldsymbol{V}_{sw} - \boldsymbol{bb} : \nabla \boldsymbol{V}_{sw} \right) + \mu^2 \boldsymbol{bb} : \nabla \boldsymbol{V}_{sw} \right] p(s) ds$$

- The adiabatic cooling effect, only lowers the total flux rather than altering the enhancement pattern.
- The adiabatic cooling effect is not responsible for the enhancement in the decay phase.

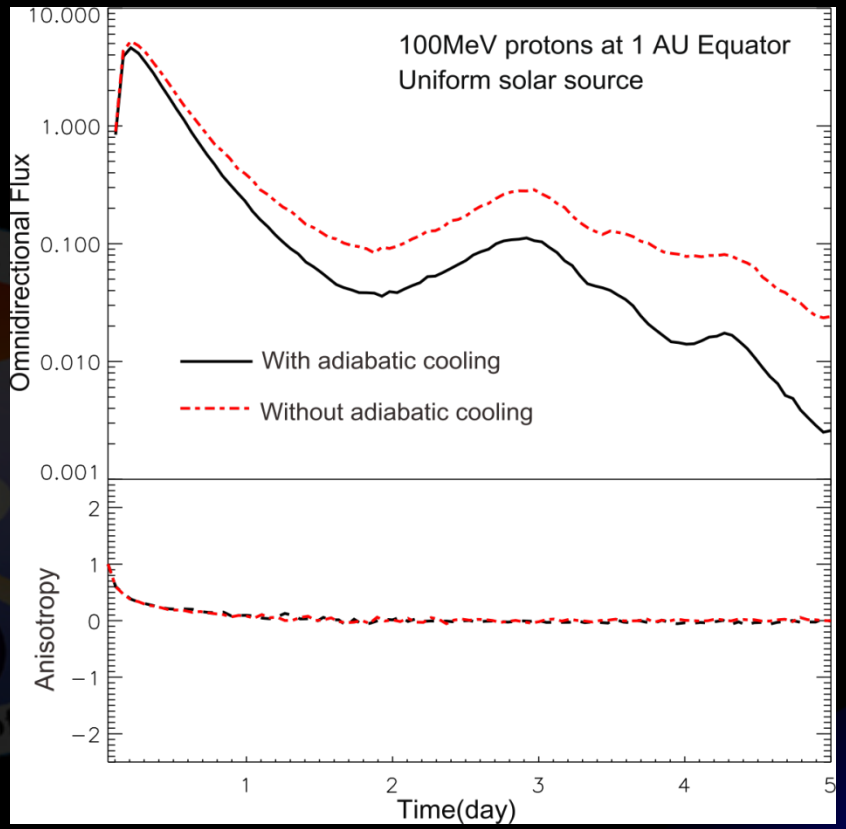

Figure 10a The comparison of omnidirectional flux and anisotropy solved with and without adiabatic cooling.

Discussion—Pitch-angle diffusion

- Pitch-angle diffusion is caused by the magnetic fluctuations, and its strength is determined by the parallel mean free path (Qin et al., 2004, Zhang et al., 2009);
- Since the influence exerted by the change of parallel diffusion coefficient is similar to that of the adiabatic cooling effect, the magnetic focusing effect is more likely to be responsible for the flux enhancement in the decay phase.

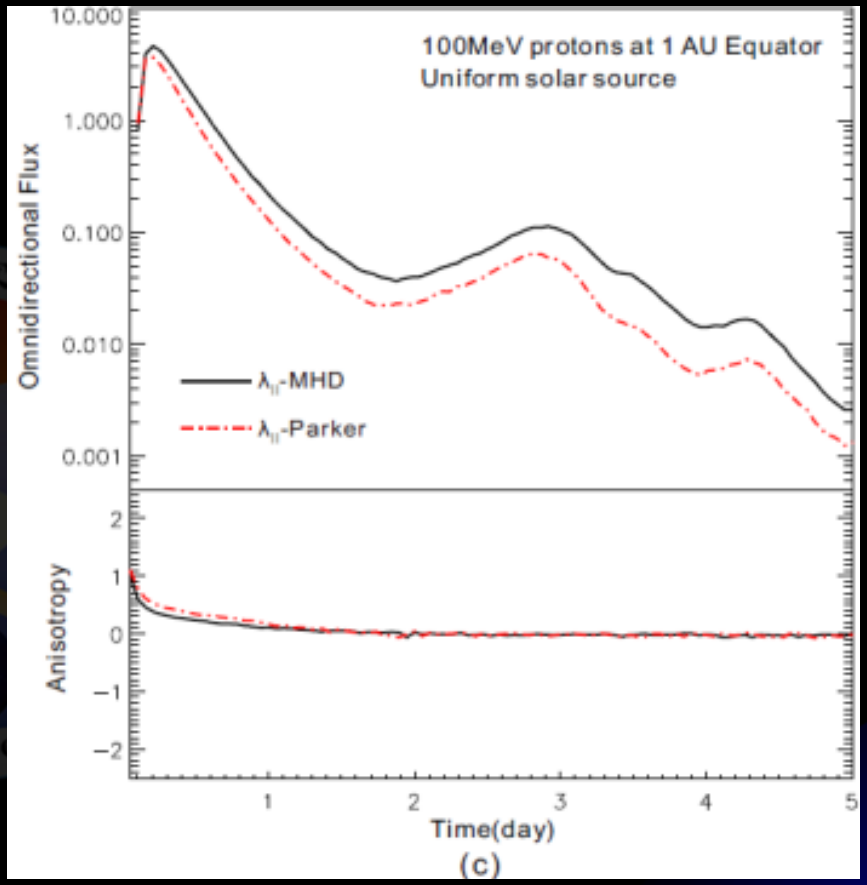

Figure 10b The comparison of omnidirectional flux and anisotropy solved with different parallel mean free paths $\lambda_{//}$.

Discussion— Magnetic focusing effect

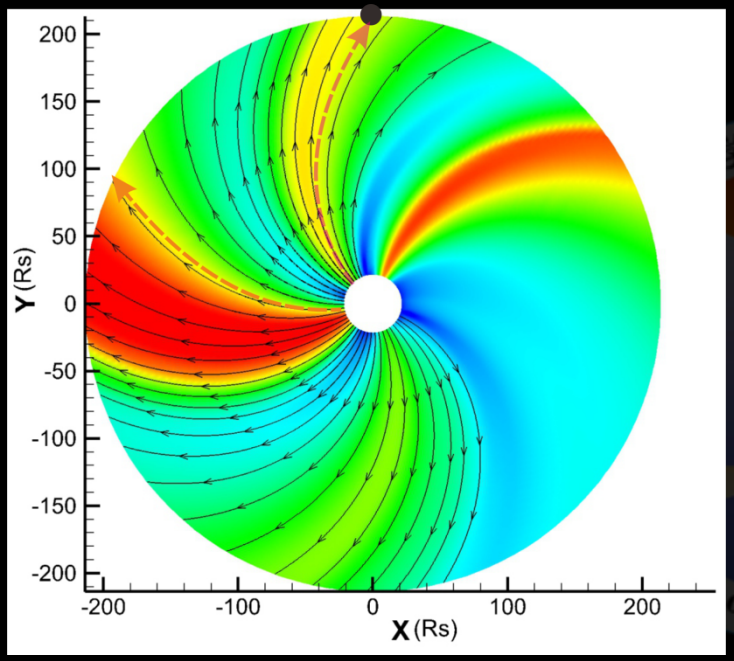

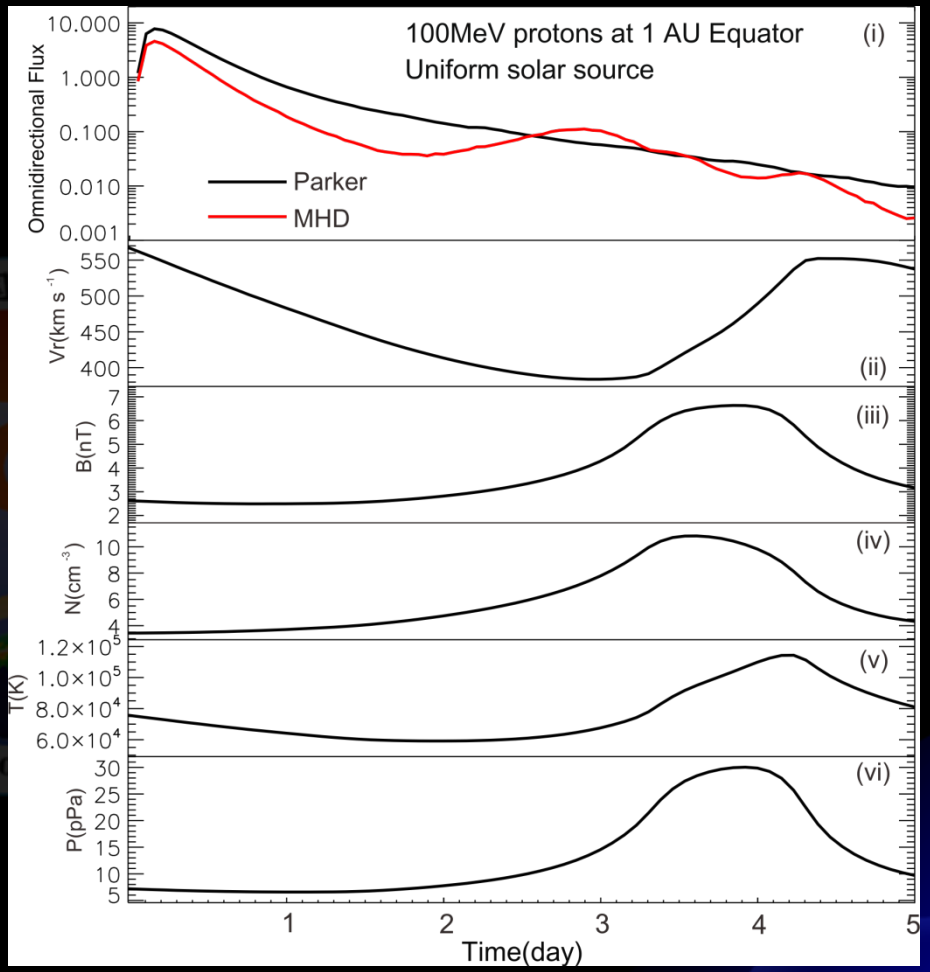

Figure 11. Illustration of omnidirectional flux with different background field and solar wind parameters under compression solar wind conditions.

Magnetic focusing effect

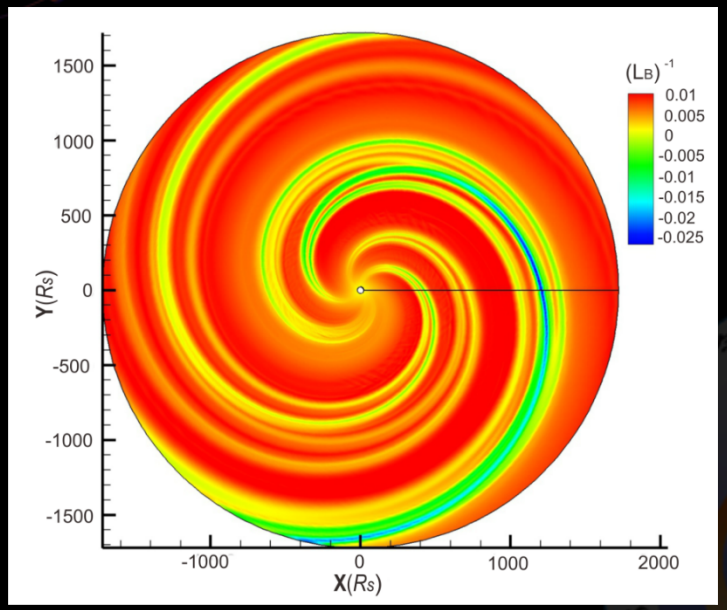

Figure 12, The $(L_B)^{-1}$ at Equator during CR2145.

- $(L_B)^{-1}$ generally describes the strength of magnetic focusing effect, and a negative value implies the focusing effect acts on the opposite direction.
- This figure shows that $(L_B)^{-1}$ varies between positive and negative values, which are different from the only positive values in Parker magnetic field.

In Parker IMF, $$\boldsymbol{b} = \boldsymbol{B}/B = \cos\beta \boldsymbol{e}_r - \sin\beta \boldsymbol{e}_\phi, \cos\beta = \frac{B_r}{B}, \sin\beta = -\frac{B_\phi}{B}$$

The focusing effect, $$\frac{(1-\mu^2)v}{2L_B} = \frac{(1-\mu^2)v\cos\beta(1+\cos^2\beta)}{2r} (\cos\beta > 0)$$ ⇒ the focusing term is not negative

In MHD IMF, $$\frac{1}{L_B} = \frac{1}{r^2}\frac{\partial}{\partial r}(r^2 b_r) + \frac{1}{r\sin\theta}\frac{\partial}{\partial\theta}(\sin\theta b_\theta) + \frac{1}{r\sin\theta}\frac{\partial}{\partial\varphi} b_\varphi$$

⇓ could be positive or negative

Correlations between ΔV_r and $(L_B)^{-1}$

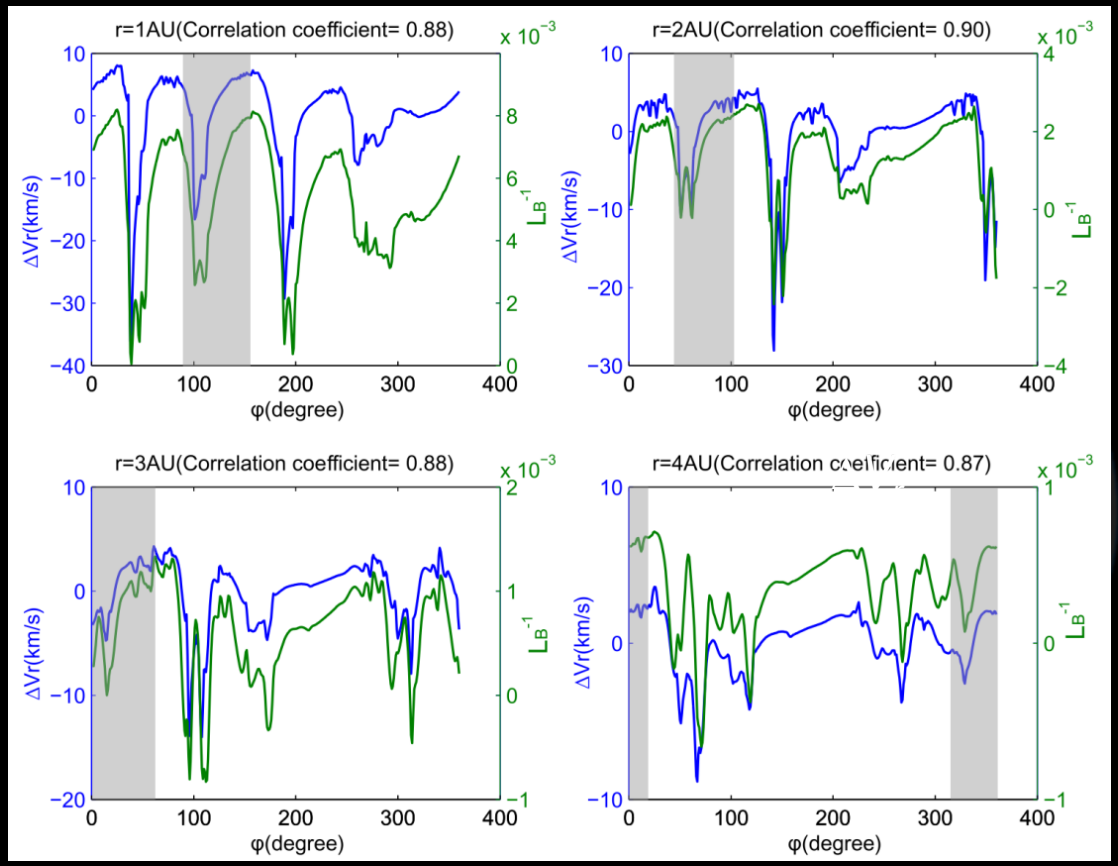

Figure 13 The correlation coefficients between ΔV_r ($\Delta V_r = V_i - V_{i+1}$) and $(L_B)^{-1}$ at different radial distances locations during CR2145. The blue lines and the green lines represent ΔV_r and $(L_B)^{-1}$, respectively. The gray shaded areas represent the variation of **$(L_B)^{-1}$** and **ΔV_r** in the simulation region.

- All the correlation coefficients between them are above 0.87, which indicates a strong correlation between them.
- The compression regions, as suggested by the **decreased ΔV_r** are generally corresponds to **small $(L_B)^{-1}$** , implying the **magnetic focusing effect** relates closely to the **compression regions**

Magnetic focusing effect

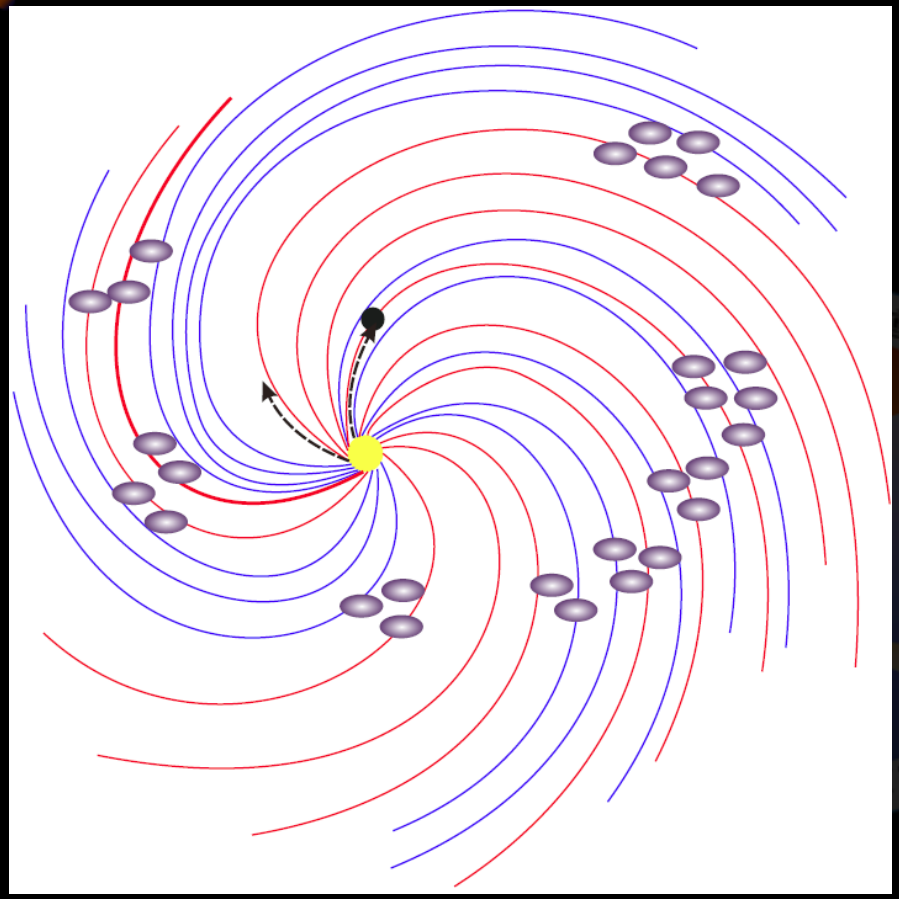

- When the particles transport in the compression regions, magnetic focusing effect could scatter some particles back like a mirror as $(L_B)^{-1}$ value becomes small.
- The particles may also be reflected since an opposite directional focusing effect happens as $(L_B)^{-1}$ becomes negative.
- Therefore the observer detects a flux enhancement.

Figure 14. Cartoon to show the possible processes of magnetic focusing effect. The red and blue lines represent the positive and negative values of $(L_B)^{-1}$, respectively. The purple balls that mainly distribute between the red and blue lines infer the strong compression regions that may reflect the particles back. The black dash lines with arrow and the black ball show the region that sweeps over the observer at 1 AU and the observation point

An event observed on March, 2011 by STEREO A

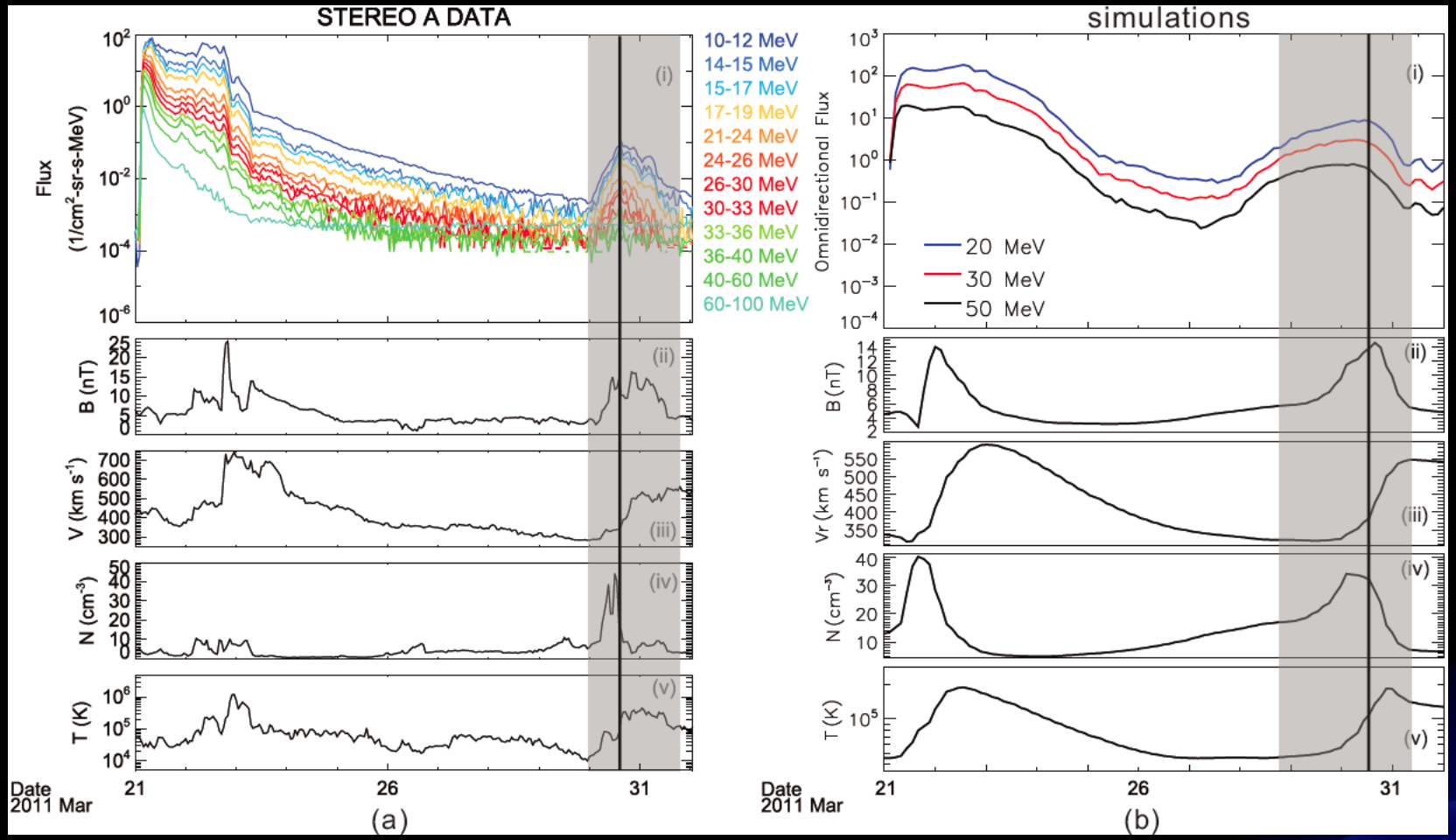

Figure 15 (a) STEREO A observations. (b) Simulation results during the corresponding observation time. The shaded region represents the compression region. From top to bottom, the panels show the flux of energetic particles, magnetic field strength, proton velocity, density and temperature.

Summary

- With the MHD-SEP model, we study the influence of interplanetary structures, such as **compression regions**, on SEP time intensity profiles.
- We find that the particles have a similar behavior in uncompressed solar wind with that in Parker spiral magnetic field, but the **omnidirectional flux of SEP has an enhancement in the decay phase in compression regions**.
- Our simulation results focus on transport process, exclude the acceleration mechanisms and find that the **magnetic focusing effect is the main reason that leads to the flux enhancement in the decay phase**.
- A SEP event with a compression region on March 21-31 2011 event was simulated with our MHD-SEP model, and our simulation results could qualitatively **reproduce the pattern of the flux enhancements during the decay phase** for this event.

Thanks